Journal of Sustainability Science and Management 2009 Volume 4 (2): 27-35

STUDIES ON THE SEA-SURFACE CURRENT-CIRCULATION PATTERN IN THE SOUTH CHINA SEA DERIVED FROM SATELLITE ALTIMETRY

NURUL HAZRINA IDRIS, MOHD IBRAHIM SEENI MOHD AND ARTHUR. P. CRACKNELL

Department of Remote Sensing, Faculty of Geoinformation Science and Engineering, Universiti Teknologi Malaysia, 81310 Skudai, Johor Darul Takzim, Malaysia.

** Corresponding author e-mail address: nurulhazrina@ utm.my and mism@ utm.my*

Abstract: Radar altimeters flown in space are very useful tools for providing information about the ocean globally and continuously, including the study of surface currents. This research is concerned with the geostrophic currents in the South China Sea. Maps of geostrophic current-circulation patterns are produced for four periods, which are the northeast monsoon, the southwest monsoon and the inter-monsoon periods for April and October in 2004 and in 2005. The main data utilised are the sea-level anomaly from Jason-1 satellite altimetry data. To compute the geostrophic current velocity, the geostrophic equations were used. In order to validate the derived surface current, the correlation coefficient with field measurement data was determined. The field data are measured using Lagrangian buoys under the Data Buoy Cooperation Panel programme (DBCP) and also from the Japanese Oceanography Data Centre (JODC). In this study, it was found that the correlation of geostrophic current speed and direction is reasonable with coefficient of 0.9 and 0.7, respectively. As far as the geostrophic current-circulation pattern is concerned, the current in the South China Sea was pushed southward during the northeast monsoon and reversed during the southwest monsoon period. In addition, during the northeast and southwest monsoon, the water moved in anticlockwise and clockwise directions, respectively. This leads to the conclusion that the geostrophic circulation pattern can be monitored from satellite altimetry data.

KEYWORDS: Altimetry, Geostrophic current, South China Sea, Surface circulation pattern.

Introduction

Space-based mapping systems like radar altimetry provide synoptic measurements of the Earth's ocean. The capability of radar altimetry to provide accurate information of ocean properties has been proved [Challenor et al., 1996] whereby the accuracy of each height measurement can achieve up to 4 cm [Fu and Cazenave, 1994]. Generally, satellite altimeter observations of sea level, coupled with knowledge of the marine geoid (the gravitational equipotential closest to the time-averaged sea-surface height), provide global information on the ocean surface. Basically, geostrophy is the term used to describe the situation when there is equilibrium between the horizontal pressure-gradient force in the ocean and the Coriolis force. For currents at the sea surface, the horizontal pressure gradient is proportional to the sea-surface slope measured relative to the equipotential surface [Robinson, 2004].

In the work described in this paper, satellite altimetry data was used to study the geostrophic currents in the South China Sea. The South China Sea is a large marginal sea situated at the western side of the tropical Pacific Ocean. It occupies an area of 3.4 x 10^6 km^2 from the equator to 23º north and from 99º east to 121º east [Chung et al., 2000]. The area of the South China Sea is shown in Figure 1. In this study, surface currents between the equator and 2º north are not considered because the geostrophic current equations are not valid in this region. This is because the Coriolis

force effects in this region are very weak. Therefore, there is no equilibrium between the horizontal pressure-gradient force and the Coriolis force.

Numerous investigators have studied the surface currents in the South China Sea region. For example, Nurul Hazrina and Mohd Ibrahim [2007] studied the sea-surface current-circulation pattern in the South China Sea derived from satellite altimetry. Peter et al. [1999] studied dynamical mechanisms for the South China Sea seasonal circulation and thermohaline variability. Mao et al. [1999] studied the geostrophic current-circulation pattern using Geosat altimeter data. They found that the general circulation pattern of the South China Sea is anticyclonic in summer and cyclonic in winter. Soong et al. [1995] studied the surface-circulation pattern in the South China Sea using TOPEX/ POSEIDON altimeter data. They found a large cyclonic eddy appeared in the northern part of the South China Sea in January 1994.

Since the capability of radar altimetry to provide the surface current has been established, this study is concerned with the geostrophic current in the southern part of the South China Sea during four monsoon periods, which are the northeast monsoon (NE), the southwest monsoon (SW) and the inter-monsoon periods of April (IMA) and October (IMO) in 2004 and in 2005. The area of interest is from 2º north to 15º north and 100º east to 120º east. The main data utilised in this study includes the sea-level anomaly from satellite altimetry. According to Robinson (2004), geostrophic current equations ignore the acceleration of the flow. Basically, the acceleration dominates if the horizontal dimensions are less than roughly 50 km and duration is less than a few days. Acceleration is negligible, but not zero, over longer times and distances. In order to eliminate the acceleration of the flow, sea-level anomaly data was gridded into 1 degree latitude and longitude bins, since a 1 degree spatial interval is around 100 km. In addition, this data was corrected for the effects of atmospheric refractions i.e. wet tropospheric, dry tropospheric and ionosperic effects, tides and ocean waves. In order to remove the geoid undulation effects, the sea-level anomaly data was added to the mean dynamic topographic data. This produced the sea-surface height data relative to the geoid. As far as the validation of the results are concerned, the sea-surface current speed and direction from field measurements were used. The data is available via the Coriolis ftp site; ftp://ftp.ifremer.fr/ifremer/coriolis/lagrangian_buoy and Japanese Organisation Data Centre (JODC) site; http://jdoss1.jodc.go.jp/cgi-bin/1997/ocs.

Geostrophic Current Equations

In this study, the geostrophic current is calculated using the geostrophic current-velocity formula [Robinson, 2004,] [Chung et al., 2000],

$$u = -g / f (d\zeta /dy) \quad (1)$$

$$v = g / f (d\zeta / dx) \quad (2)$$

$$V = \sqrt{(u^2 + v^2)} \quad (3)$$

$$\theta = tan^{-1} (v / u) \quad (4)$$

$$f = 2\Omega \cos \varphi \quad (5)$$

$$x = R (\lambda - \lambda_0) \cos \varphi \quad (6)$$

$$y = R\varphi \quad (7)$$

where u and v are the geostrophic current in zonal and meridional direction, respectively, V is the geostrophic current amplitude and θ is the geostrophic current direction, g is the gravitational acceleration, f is the Coriolis force, ζ is the sea-surface height relative to the geoid, x and y is the local east coordinate and local north coordinate, respectively, Ω is the Earth rotation rate = 7.27 x 10^{-5} s^{-1}, φ is the latitude in radians, R is the Earth radius = 6371 kilometers and λ is the longitude in radians.

Implementation of The Geostrophic Current Equations

Geostrophic current equations in equation 1 and 2 can be written as,

$$u_g = - \frac{g}{f} \frac{(h_2 - h_1)}{(x_2 - x_1)} \quad (8)$$

$$v_g = \frac{g}{f} \frac{(h_3 - h_1)}{(y_2 - y_1)} \quad (9)$$

where u_g and v_g are zonal x and meridional y components of the geostrophic velocity, respectively, g is the gravitational acceleration, f is the Coriolis parameter, h is the corrected sea-level anomaly, x is local east coordinate and y is local north coordinate.

In Figure 2, nodes represent the sea-level anomaly at coordinate x_i, y_i. By calculating the slope of the sea-level anomaly ($h_2 - h_1$) and the distance of local east coordinate ($x_2 - x_1$) which were then applied to equation 8, the geostrophic current in zonal direction for coordinate x_1, $y_1$was obtained. By calculating the difference of the sea-level anomaly ($h_3 - h_1$) and the local north distance ($y_2 - y_1$) which were then applied to equation 9, the geostrophic current in meridional direction for coordinate x_1, y_1 was obtained. In order to get the resultant of geostrophic current speed and direction for that location, equations 3 and 4 were used.

Geostrophic Current Circulation Pattern

The circulation patterns of geostrophic currents over the four monsoon periods in 2004 and in 2005 are shown in Figure 3. These are presented in vector plots where the arrows represent the directions of geostrophic current and the length of arrows represent the magnitudes of the surface current in cm s^{-1}. In this study, the surface-current pattern and the circular movement of water will be monitored.

As far as the geostrophic current-circulation pattern is concerned, during IMA 2004 (Figure 3 (a)), surface water on the coast of Borneo Island moves along the coast towards the south. However, on the east coast of Peninsular Malaysia and on the east coast of Indochina, the surface current moves along the coast towards the north. This creates a large clockwise circulation of surface current in the South China Sea. In 2005 (Figure 3 (b)), there is no specific surface current-circulation pattern can be detected. However, we found that the surface water on the coast of Peninsular Malaysia moves in the opposite direction of surface current in 2004. On the coast of Borneo Island, surface water moves along the coast towards the south.

During IMO 2004 (Figure 3 (c)), surface water on the east coast of Indochina and on the east coast of Peninsular Malaysia moves towards the south along the coast. On the coast of Borneo Island, a clockwise surface water circulation pattern was detected. In 2005 (Figure 3 (d)), it was

found that surface water moves towards the south in the most of the area. A clockwise surface water-circulation pattern also was detected on the coast of Borneo Island.

During the SW monsoon periods (Figure 3 (e) and Figure 3 (f)), surface water moves clockwise in most of the area. Over the periods, surface water on the west coast of Palawan Island and on the coast of Borneo Island moves southward. On the east coast of Peninsular Malaysia and on the east coast of Indochina, surface water moves towards the north along the coast. This creates a huge clockwise surface-current circulation over the sea.

As far as the surface water-circulation pattern during NE monsoon periods is concerned, generally surface water moves southwards in most of the area (Figure 3 (g) and Figure 3 (h)). In 2004, surface water on the west coast of Palawan Island and on the east coast of Indochina moves towards the south along the coast. In 2005, surface water on the coast of Borneo Island, on the east coast of Peninsular Malaysia and on the south coast of Indochina moves towards the south. Besides, it was found that surface water on the northern part of the sea deflects to the right.

Results Analysis

In order to assess the accuracy of derived geostrophic current, correlation and descriptive statistical analysis was carried out. 50 sample points were used in the analysis. The distribution of sample points was represented in Figure 4. (Some points have the same geographical coordinates since the field-measurement values were obtained in 2-year periods).

It was found that the correlation of geostrophic current speed and direction is reasonable with correlation coefficients of 0.9 and 0.7, respectively. Figure 5 and Figure 6 represent the graph of relationship between derived value and field measurement for speed and direction, respectively. In addition, the means and the standard deviations of the derived geostrophic current are not significantly different from the means and the standard deviations of the field-measurement values. Table 1 illustrates the means and the standard deviations of the derived geostrophic current and the field-measurement values. Table 1 shows that mean ± standard deviation of the derived geostrophic current speed and direction are (14 ± 13) cm s^{-1} and (198 ± 92)º whereas mean ± standard deviation of the field-measurement speed and direction are (15 ± 10) cm s^{-1} and (194 ± 88)º.

Based on the analysis of results, we found that the general sea-surface current-circulation pattern can be detected using the geostrophic current equations from the satellite altimetry data with reasonable accuracy. Since the spatial resolution of the satellite altimetry data used in this study is not really precise, a smaller scale of current phenomena i.e. eddies cannot be detected accurately. Besides the limitation of satellite data, other factors that contribute to the movement of sea-surface current also should be considered i.e. wind effects and tidal variations, in order to improve the accuracy.

Conclusion

Geostrophic currents can be estimated using sea surface-height data derived from a satellite altimeter. It was found that the derived surface current is reasonably well correlated with the field data whereby the correlation coefficient for speed and direction is 0.9 and 0.7, respectively. In addition, the means and the standard deviations of the derived geostrophic current are not significantly different from the field-measurement values. This leads to the conclusion that the surface current in the South China Sea can be estimated from satellite altimetry data using the geostrophic current equations with reasonable accuracy. However, only general circulation patterns can be monitored since there is a limitation on the satellite data used.

Acknowledgement

The Jason-1 satellite data were produced by SSALTO/DUACS and distributed by Archiving, Validation, and Interpretation of Satellite Data in Oceanography (AVISO), with support from French Space Agency Centre National d'Etudes Spatiales (CNES). The field measurement data were provided by Malaysian Meteorological Services, Japanese Organisation Data Centre and Coriolis Data Centre.

References

Challenor P. G. , J. F. Read, and R. T. Tokmakin. (1996). Measuring surface currents in Drake Passage from satellite altimetry and hydrography. *Journal of Physical Oceanography,* 26, pp 2748-2758.

Chung R. H., Q. Zheng, Y. S. Soong, J. K. Nan, and H. H. Jian. (2000). Seasonal variability of sea surface height in the South China Sea observed with TOPEX/Poseidon altimeter data. *Journal of Geophysical Research,* 105, pp 13,981-13,990.

Fu, L. L., and A. Cazenave. (1994). *Satellite altimetry and earth sciences: A handbook of techniques and applications,* International Geophysics Series, Vol. 69, San Diego, CA: Academic Press,

Mao Q. W., P. Shi, and Y. Q. Qi. (1999) Sea surface dynamic topography and geostrophic current over the South China Sea from Geosat altimeter observation. *Acta Oceanologica Sinica,* 21, pp 11- 16 (in Chinese with English abstract).

Nurul Hazrina Idris and Mohd Ibrahim Seeni Mohd. (2007), Sea Surface Current Circulation Pattern in the South China Sea Derived from Satellite Altimetry. Proceeding of Asian Conference on Remote Sensing, Kuala Lumpur, Malaysia.

Peter C. C. , L. E. Nathan, and Chenwu Fan. (1999). Dynamical mechanism for the South China Sea seasonal circulation and thermohaline variability. *Journal of Physical Oceanography,* 29, pp 2971- 2989.

Robinson I. S. (2004). *Measuring the oceans from space: Principles and methods of satellite oceanography,* Springer, Praxis Publishing, Chichester, UK,

Soong Y. S., J. H. Hu, C. R. Ho, and P. P. Niiler, (1995) Coldcore eddy detected in the South China Sea. *EOS,* 76, , pp 345 – 347.

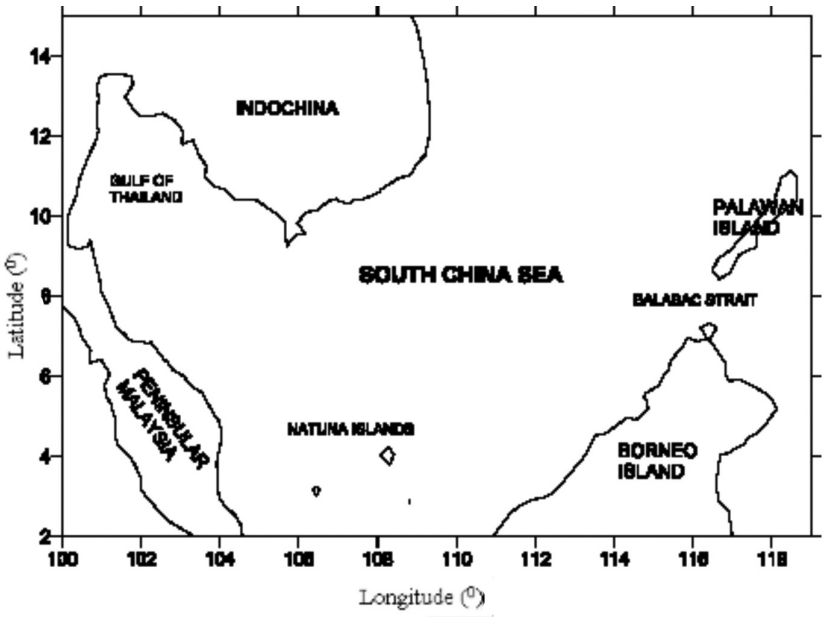

Figure 1. The South China Sea region.

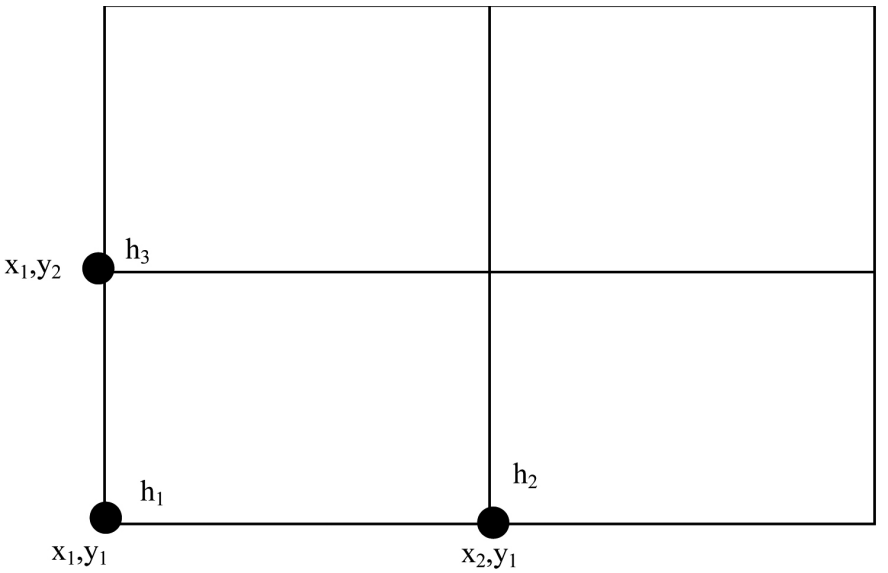

Figure 2. Illustration of grid to implement the geostrophic current equations.

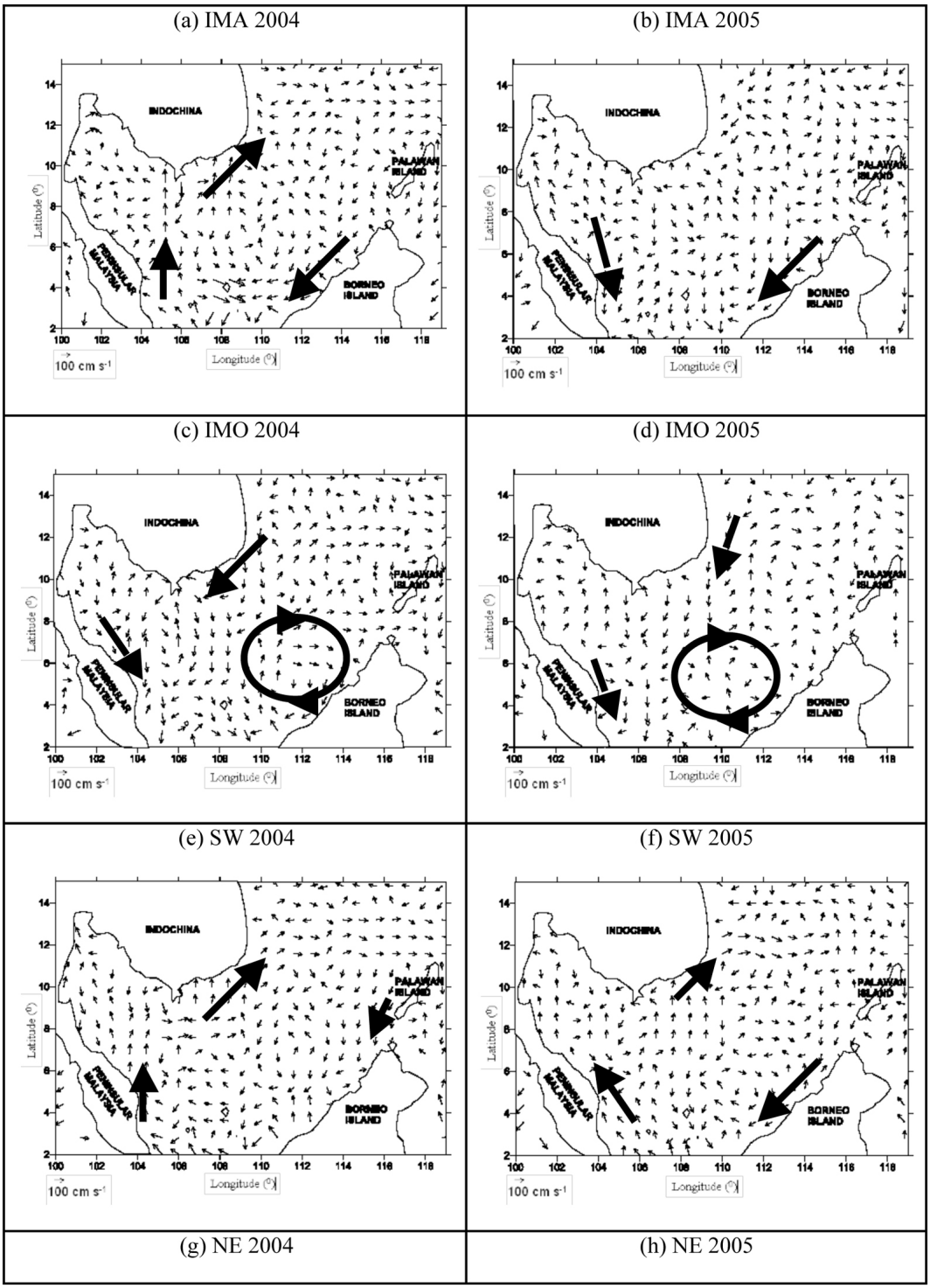
(a) IMA 2004
(b) IMA 2005
(c) IMO 2004
(d) IMO 2005
(e) SW 2004
(f) SW 2005
(g) NE 2004
(h) NE 2005
INDOCHINA
PALAWAN ISLAND
PENINSULAR MALAYSIA
BORNEO ISLAND
Latitude (°)
Longitude (°)
100 cm s-1

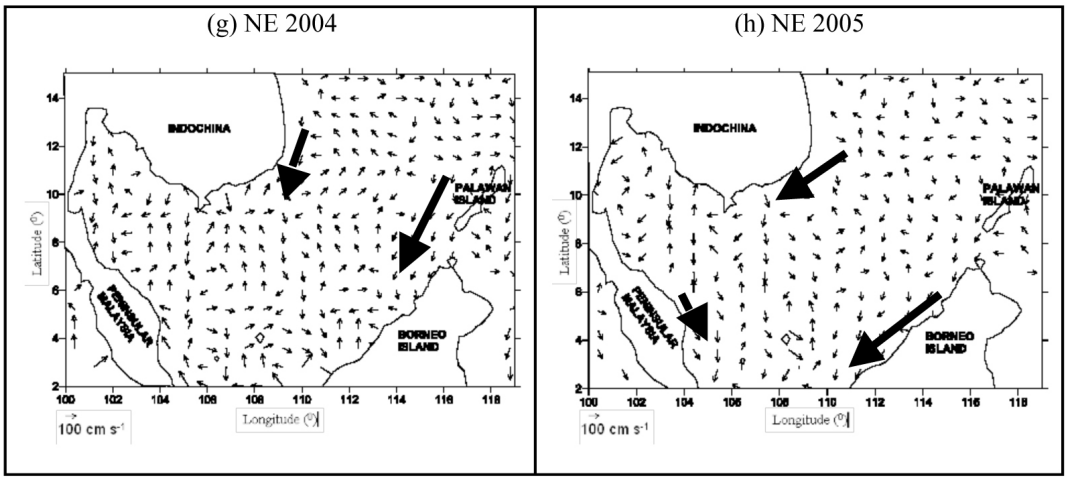

Figure 3.Geostrophic current circulation pattern on (a) IMA 2004, (b) IMA 2005, (c) IMO 2004, (d) IMO 2005, (e)SW 2004, (f) SW 2005, (g) NE 2004 and (h) NE 2005.

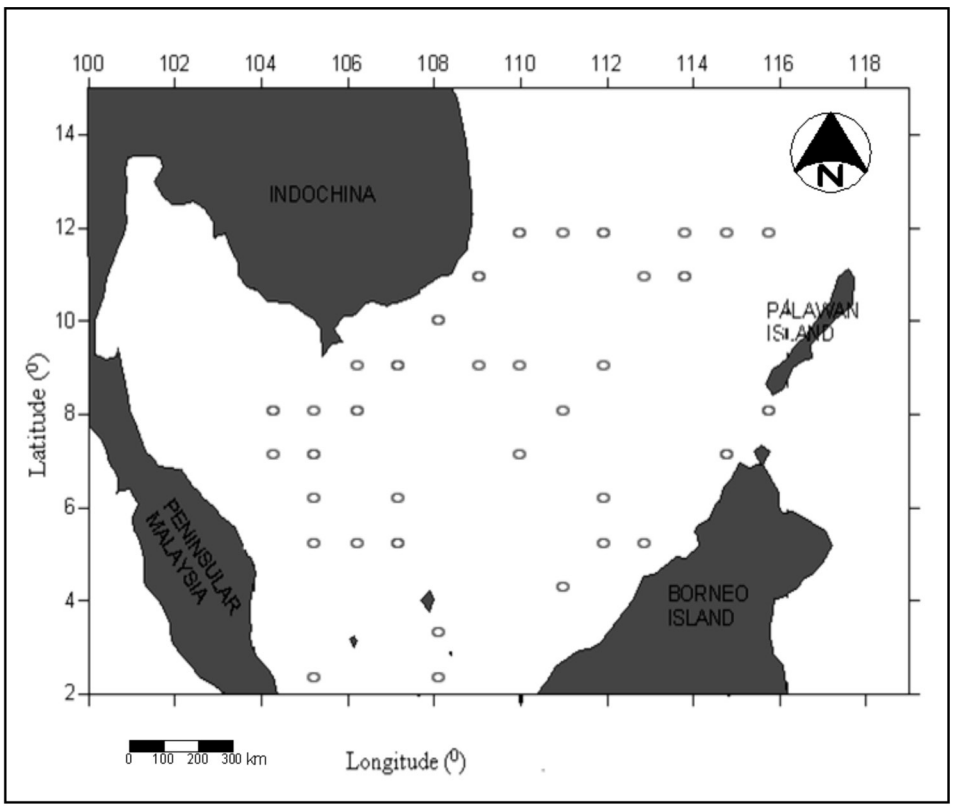

Figure 4. Distribution of sample points used in the analysis.

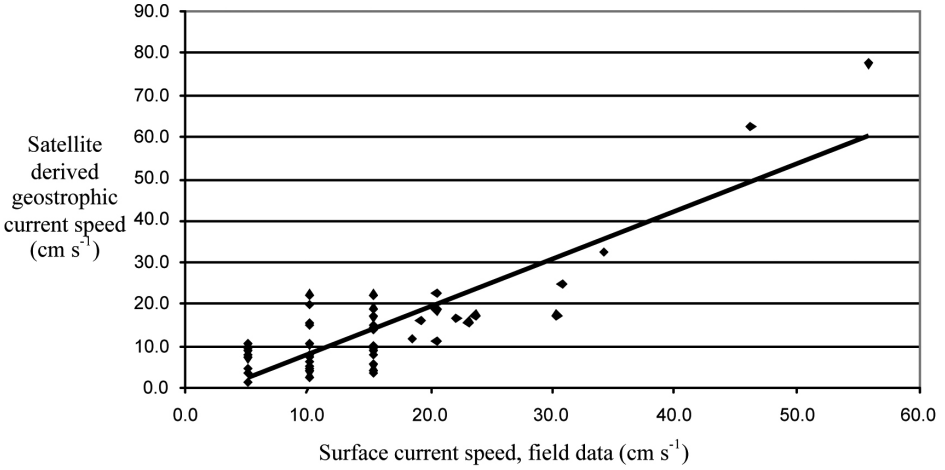

Figure 5. Relationship between field data and geostrophic current speed.

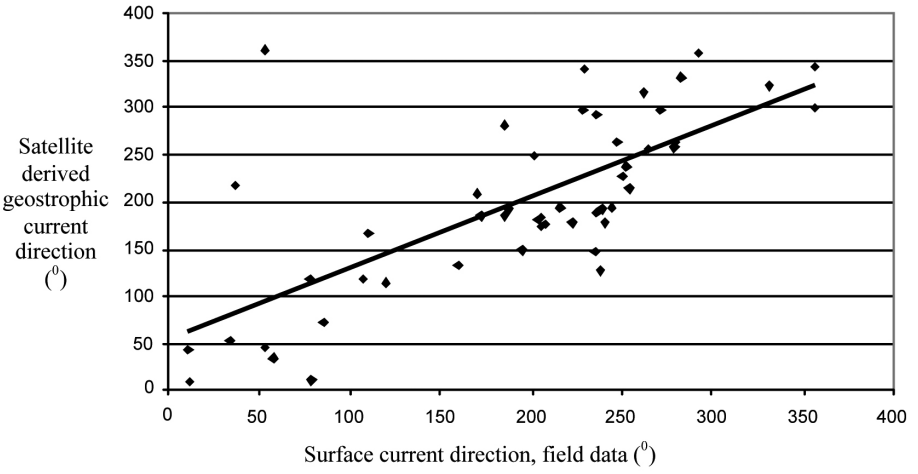

Figure 6. Relationship between field data and geostrophic current direction.

Table 1. Means and standard deviations of sea surface current.

	Field measurement values (cm s^{-1})		Satellite derived geostrophic current (cm s^{-1})	
	Speed (cm s^{-1})	Direction (^{0})	Speed (cm s^{-1})	Direction (^{0})
Mean	15	194	14	198
Standard deviation	10	88	13	92